Acta Crystallographica Section B
Structural Science
ISSN 0108-7681

Sensitive detection of mirror symmetry by CBED applied to $LaAlO_3$ and $GdAlO_3$

Daniel M. Jones

School of Physics, The University of Western Australia, Crawley 6009, Australia

Correspondence e-mail: bill@physics.uwa.edu.au

Received 7 September 2006
Accepted 30 October 2006

Convergent-beam electron diffraction (CBED) patterns tilted away from major zone axes have been used to re-examine the space groups of $LaAlO_3$ and $GdAlO_3$ perovskites. The higher-order Laue zones (HOLZ) in CBED patterns at such tilted orientations have been found to have high sensitivity to the presence of mirror symmetry. This sensitivity has enabled the space group of $LaAlO_3$, previously claimed to be cubic ($Fm\bar{3}c$), to be confirmed as rhombohedral $R\bar{3}c$ by CBED. It is clear that patterns of sufficient tilt will be more sensitive for distinguishing between screw axes and glide planes than the observation of HOLZ deficit lines in zero-order Laue zone reflections. No symmetry degrading effects due to the influence of tilted crystal surfaces could be observed.

1. Introduction

It is well established that convergent-beam electron diffraction (CBED) is a reliable and sensitive technique for symmetry determination. Systematic approaches to the solution of space groups have been developed and these are well summarized in *International Tables for Crystallography*, Vol. B (Goodman, 2001). A range of examples of symmetry determination, which emphasize the multiple scattering aspects of CBED, are beautifully presented in the books published by Tanaka & Terauchi (1985) and Tanaka *et al.* (1988).

In the present work, the established technique of symmetry analysis at exact zone axes was found to have insufficient sensitivity to determine the space group of $LaAlO_3$. This led to the use of patterns tilted away from the exact zone axis for the purpose of mirror or glide mirror symmetry determination.

The space group of $LaAlO_3$ has been the subject of some dispute following a CBED study by Yang *et al.* (1991). Their study used exact zone-axis orientations and suggested that the structure was face-centred cubic with $Fm\bar{3}c$ symmetry. The authors claimed to have observed a zone axis with $4mm$ point-group symmetry in their CBED data, clearly inconsistent with the more commonly accepted rhombohedral structure (see §2). They concluded that the $R\bar{3}c$ symmetry reported in other studies was deceptive owing to the coexistence of the cubic ($Fm\bar{3}c$) phase with lower-symmetry phases within the same crystal. These reports led to the present re-examination of $LaAlO_3$ using the more definitive method of tilting which is described below.

The sensitivity of CBED in detecting small deviations from mirror symmetry, whilst appreciated by some who are familiar with the method, has attracted little attention in the literature.[1] The present study shows that high sensitivity to mirror

[1] Here mirror symmetry can also refer to glide mirror symmetry. It is also assumed that symmetry-reducing influences due to strain and crystal defects have been avoided.

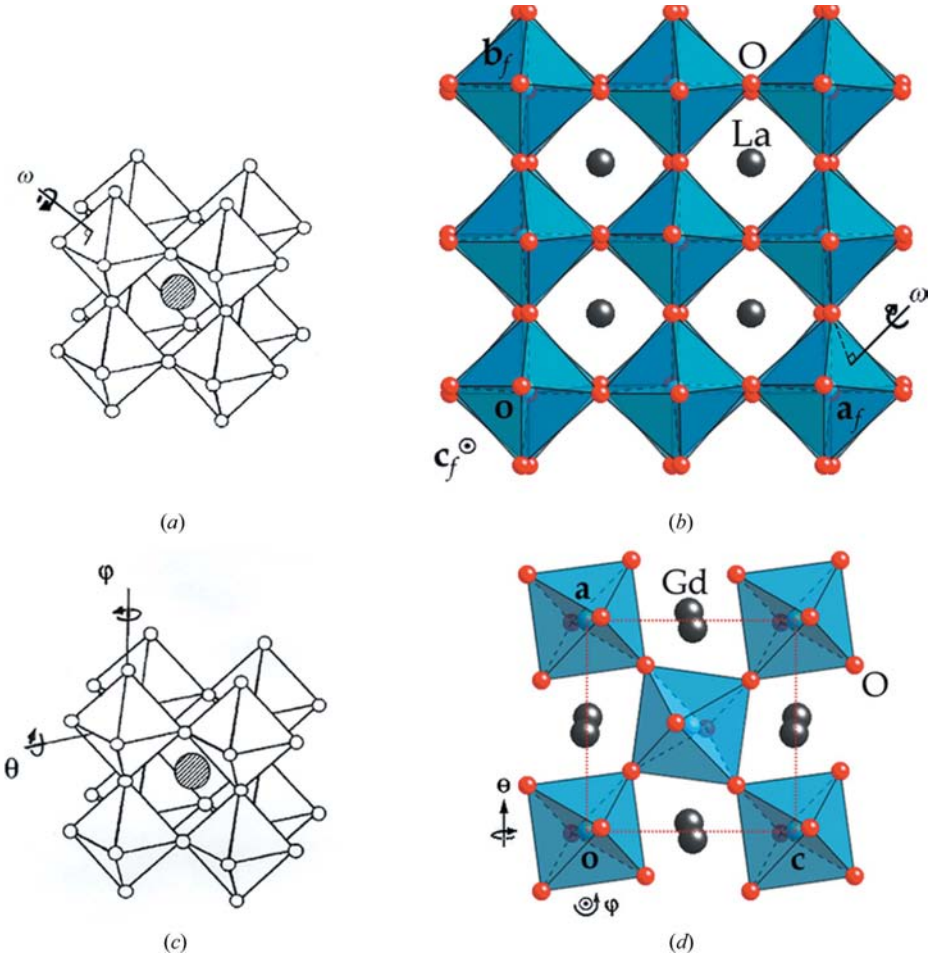

Figure 1
(*a*) Ideal cubic perovskite structure. The AlO_6 tilt (ω) that occurs in the rhombohedral structure is shown schematically. (*b*) The $R\bar{3}c$ structure of $LaAlO_3$ (atom positions; Howard *et al.*, 2000). This is viewed with respect to the face-centred, pseudo-cubic axes ($\mathbf{a}_f$, $\mathbf{b}_f$, $\mathbf{c}_f$) that are simply related to the primitive rhombohedral axes (see Moreau *et al.*, 1970). Here the pseudo-cubic, interaxial angle is 90.1°. (*c*) Schematic illustration of the AlO_6 tilts (θ and φ) that occur in the $GdAlO_3$, *Pnma* structure, shown here with respect to the ideal cubic structure. (*d*) *Pnma* structure of $GdAlO_3$ (atom positions; du Boulay *et al.*, 2004), viewed along the orthorhombic **b** axis.

symmetry can be attained by the direct observation of higher-order Laue zone (HOLZ) reflections at orientations tilted away from an exact zone axis. The reason for this sensitivity can be understood from the following. Most workers have emphasized the use of diffraction symmetries observed in zero-order Laue zone (ZOLZ) patterns taken at exact zone axes. In such cases HOLZ scattering (observed either as fine-deficit line detail in the ZOLZ or as the HOLZ reflections themselves) is observed against a background of strong ZOLZ scattering and this background decreases the sensitivity of the HOLZ observation. By tilting the crystal a few degrees away from the exact zone axis, the intensity of the HOLZ reflections at smaller scattering angles is increased. Furthermore, after tilting, inelastic scattering, which is a maximum at the zone axis, is often reduced. These conditions greatly increase the sensitivity of the HOLZ observation as lower-order HOLZ reflections may now be viewed directly against little or no background. These conditions also allow for a better assessment of the effect of misorientation on the resulting symmetry information.

In the work reported here, mirror symmetry has been tested by tilting the crystal $\sim 5^\circ$ away from the zone axis about the normals of the proposed mirror planes. The conditions described above then allow the presence or absence of mirror symmetry in the CBED data to be judged to a very high level of rigour. Subsequently in this paper it is convenient to refer to this technique as the small tilt method.

In addition to $LaAlO_3$, the orthorhombic (*Pnma*) structure of $GdAlO_3$ has also been examined using tilted CBED patterns. This well characterized structure (see §2) contains two glide mirrors and one mirror plane, and allowed the tilt method to be tested in cases where perfect mirror symmetry is known to exist.

2. Structural background

The rare-earth aluminates $RAlO_3$ (R = La, ...Lu) are a series of perovskite materials that have attracted attention because of their dielectric properties (Cho *et al.*, 1999) and, in the case of $LaAlO_3$, their use as a superconductor substrate (Berkstresser *et al.*, 1991). Across the series two distinct structural phases exist at room temperature. For $R \leq$ Nd the structure is widely regarded as rhombohedral $R\bar{3}c$ (Derighetti *et al.*, 1965), while for $R \geq$ Sm the structure is orthorhombic *Pnma* (Geller & Bala, 1956; Dernier & Maines, 1971). Both these structures derive from the ideal cubic perovskite structure ($Pm\bar{3}m$) *via* rotations of corner-linked AlO_6 octahedra (Glazer, 1972).

In the rhombohedral model of $LaAlO_3$ the AlO_6 octahedra rotate about one of the threefold axes of the ideal cubic structure (Fig. 1*a*). The small AlO_6 rotations in $LaAlO_3$ (ω = 5.8° at room temperature; Müller *et al.*, 1968) result in a structure that is only marginally distorted from cubic, as shown in Fig. 1*b*. Here the small movement of weakly scattering O atoms away from their ideal cubic sites is the most significant deviation from cubic symmetry. This, together with the fact that $LaAlO_3$ is susceptible to twinning (Bueble *et al.*, 1998), makes it difficult to study using single-crystal X-ray diffraction. CBED can overcome these difficulties by selecting single domain regions for study and by exploiting its sensitivity

to small symmetry changes owing to the movement of the light O atoms.

In the *Pnma* structure of $GdAlO_3$ the rotations of the AlO_6 octahedra are more involved. They are best represented by two independent tilts: θ about the [101] ideal cube direction and φ, a tilt about the [010] cube axis (see Fig. 1*c*). Fig. 1(*d*) shows the structure of $GdAlO_3$ viewed along the orthorhombic **b** axis. Of note is the coupling of the octahedron at **o** with the middle octahedron in the figure, which neatly illustrates the presence of an *a* glide with a mirror plane located at *c*/4. This symmetry element, in a well-characterized structure, provides an excellent test of the accuracy to which mirror symmetry is preserved in the tilted CBED patterns presented below.

3. Experimental

Specimens of $LaAlO_3$ were grown using a simple adaptation of the flux-growth technique of Marezio *et al.* (1970) in which La_2O_3 and Al_2O_3 was dissolved in a K_2CO_3/B_2O_3 flux, yielding rectangular, reddish brown crystals. Specimens of $GdAlO_3$ were prepared using the flux-growth technique of Wanklyn (1969), by dissolving Gd_2O_3 and Al_2O_3 in a $PbO/PbF_2/B_2O_3$ flux. The colourless $GdAlO_3$ crystals liberated from the flux were also rectangular. It is important to note that no annealing of the specimens was conducted in these preparations. In contrast, the crystals used in the CBED study of $LaAlO_3$ by Yang *et al.* (1991) were grown by the Czochralski method. In their study specimens were annealed for 'short' and 'long' times and the reported symmetry was found to be dependent on the annealing conditions.

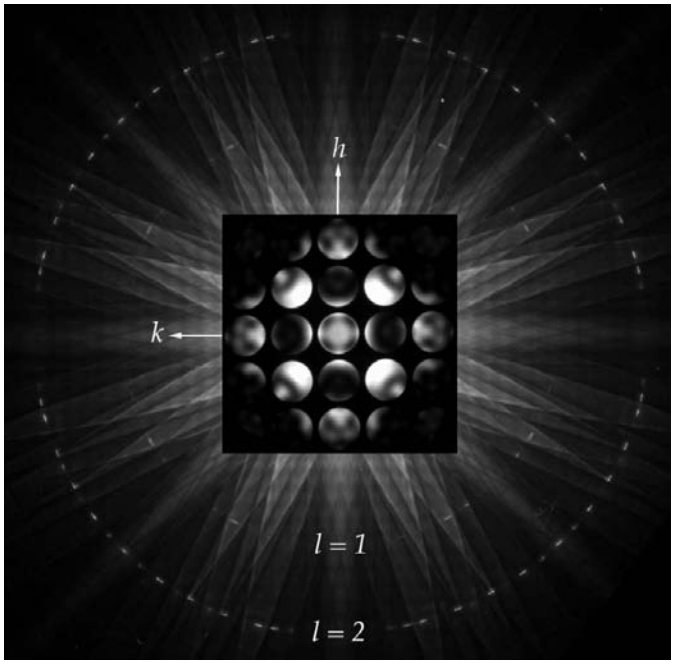

Figure 2
[001] CBED pattern of $LaAlO_3$ showing apparent 4*mm* symmetry. Only the ZOLZ (square inset) has been recorded using an image filter to remove the inelastic background and is enlarged for ease of observation. Reflection indices are expressed with respect to face-centred, pseudo-cubic axes.

In the present work a single crystal of $LaAlO_3$ or $GdAlO_3$ was lightly crushed in ethanol and the suspension deposited onto a copper specimen grid coated with holey carbon film. Both $LaAlO_3$ and $GdAlO_3$ specimens were examined in a Philips EM430 transmission electron microscope at 250 kV, using a probe size of 50 nm. Additional CBED data was obtained from $LaAlO_3$ at 300 kV using a Jeol 3000F TEM equiped with a Gatan image filter. Energy-dispersive X-ray spectra, recorded from both $LaAlO_3$ and $GdAlO_3$ specimens, showed the expected peaks, with no evidence of impurities within the limits of detection ($\sim 1\%$).

4. Results

4.1. $LaAlO_3$

Fig. 2 shows a CBED pattern, typical of many $LaAlO_3$ specimens, with the beam aligned along one of the pseudo-cubic axes. Unit-cell parameters, recovered from such patterns using the techniques of Johnson (1992), were found to be consistent with a face-centred cubic lattice [a_f = 7.57 (2) Å, α_f = 90.2 (6)°]. These values are also consistent with the rhombohedral parameters[2] obtained from powder XRD by Lehnert *et al.* (2000) [a_f = 7.582 (1) Å, α_f = 90.09 (1)°].

The ZOLZ in Fig. 2 shows convincing 4*mm* symmetry. The two HOLZ rings, l = 1 and 2, also suggest an initial 4*mm* classification. However, the 4*mm* symmetry of the l = 1 ring is less certain owing to the weak intensity of these reflections against a high inelastic background. Furthermore, slight misalignment of the electron beam (*e.g.* due to drift) can affect the appearance of these reflections, adding uncertainty to the observed symmetry.

As discussed in §1, a more sensitive way to test the four possible mirrors in Fig. 2 is to apply the small tilt method independently to each. Fig. 3(*a*) shows the case of tilting the crystal away from the [001] by $\sim 5°$ about the $\mathbf{b}_f$ axis. This reveals HOLZ arcs that contain reflections that may be compared pairwise across the h axis. Here the l = 0 arc shows good mirror symmetry, whilst the l = 1 and −1 arcs show subtle but clear mirror-symmetry breakdown. This is clearly seen in, for instance, the (7, ± 11, 1) pair of reflections from the l = 1 arc, which are illustrated in detail in Figs. 3(*b*) and (*c*).

Fig. 4 shows the result of tilting the crystal away from [001] by $\sim 5°$ about the $\mathbf{a}_f - \mathbf{b}_f$ axis. In contrast to Fig. 3, this shows convincing mirror symmetry in all the HOLZ arcs. In fact, the Gjønnes–Moodie (GM) band (Gjønnes & Moodie, 1965) in the $(\bar{9}\bar{9}\bar{1})$ reflection from the l = −1 arc shows that this is a glide mirror.

A systematic study of the four possible mirrors in Fig. 2 revealed that only the mirror with the normal $\mathbf{a}_f - \mathbf{b}_f$ was rigorously preserved. The other three mirrors are broken, with breakdown most apparent in the weak, odd-order Laue zones. This shows that the apparent 4*mm* symmetry of the [001] zone

[2] Expressed with respect to face-centred pseudo-cubic axes. All indices quoted in this paper for $LaAlO_3$ are expressed with respect to these axes.

axis is in fact only *m* symmetry and convincingly excludes the cubic ($Fm\bar{3}c$) symmetry proposed by Yang *et al.* (1991).

During this work great care was taken to confine the probe to the same region of crystal used to obtain the [001] data. This minimizes the chance of the probe drifting to another phase or twin domain, ensuring that all the diffracted intensity comes from a common single-crystal region.

4.2. $GdAlO_3$

Fig. 5 shows a CBED pattern taken from $GdAlO_3$ with the beam aligned close to the [010] orthorhombic axis. The crystal has been tilted away from the [010] orientation by $\sim 6^\circ$ about the **c** axis. In contrast to an exact zone-axis pattern, Fig. 5 has a smaller inelastic background and shows many more HOLZ reflections satisfied at smaller scattering angles. This pattern provides a sensitive test for the presence of mirror symmetry across the *h* axis.

The mirror symmetry across all HOLZ arcs in Fig. 5 is unambiguous. Furthermore, the presence of a GM band in the (11,2,0) reflection and its absence in the (6,1,0) reflection gives evidence for the extinction condition *hk0*: $h = 2n + 1$. This indicates that the mirror in Fig. 5 corresponds to an axial *a* glide in the $GdAlO_3$ structure. This symmetry element was described in §2 with reference to Fig. 1(*d*).

Using additional tilted patterns (not shown) an *n* glide with mirror perpendicular to **a** and a mirror plane perpendicular to **b** were also determined. This is consistent with the accepted space group *Pnma* (Geller & Bala, 1956).

5. Discussion

In the $R\bar{3}c$ model of $LaAlO_3$ the AlO_6 rotation displaces the O atoms from their cubic sites (see §2) and generates weak, odd-order HOLZ reflections. The observed *m* symmetry of the [001] zone axis (§4.1) is consistent with this model. It is also consistent, however, with a monoclinic (*I*2/*a*) symmetry, which Yang *et al.* (1991) proposed for a low-symmetry phase that they observed in their $LaAlO_3$ specimens annealed for a short time. To test this possibility, the same crystal used in the experiments described in §4.1 was tilted from the [001] zone axis to the [011] orientation and then tilted about the [01$\bar{1}$] vector. This revealed a *second* mirror line in the CBED data, distinct from that observed in Fig. 4, and therefore excluded monoclinic symmetry. In fact, the work reported here is only part of a complete space-group determination that found the CBED data fully consistent with $R\bar{3}c$ symmetry. This included, rigorous observation of a threefold axis, a $\pm H$ test (Goodman, 2001) showing good evidence for centrosymmetry and further observation of GM bands in the (*hhl*) reflections confirming the *c* glide.

The $Fm\bar{3}c$ symmetry observed by Yang *et al.* (1991) was based upon symmetries observed in ZOLZ patterns. It is to be noted that in the $R\bar{3}c$ description of $LaAlO_3$, scattering into even-order reflections is dominated by the

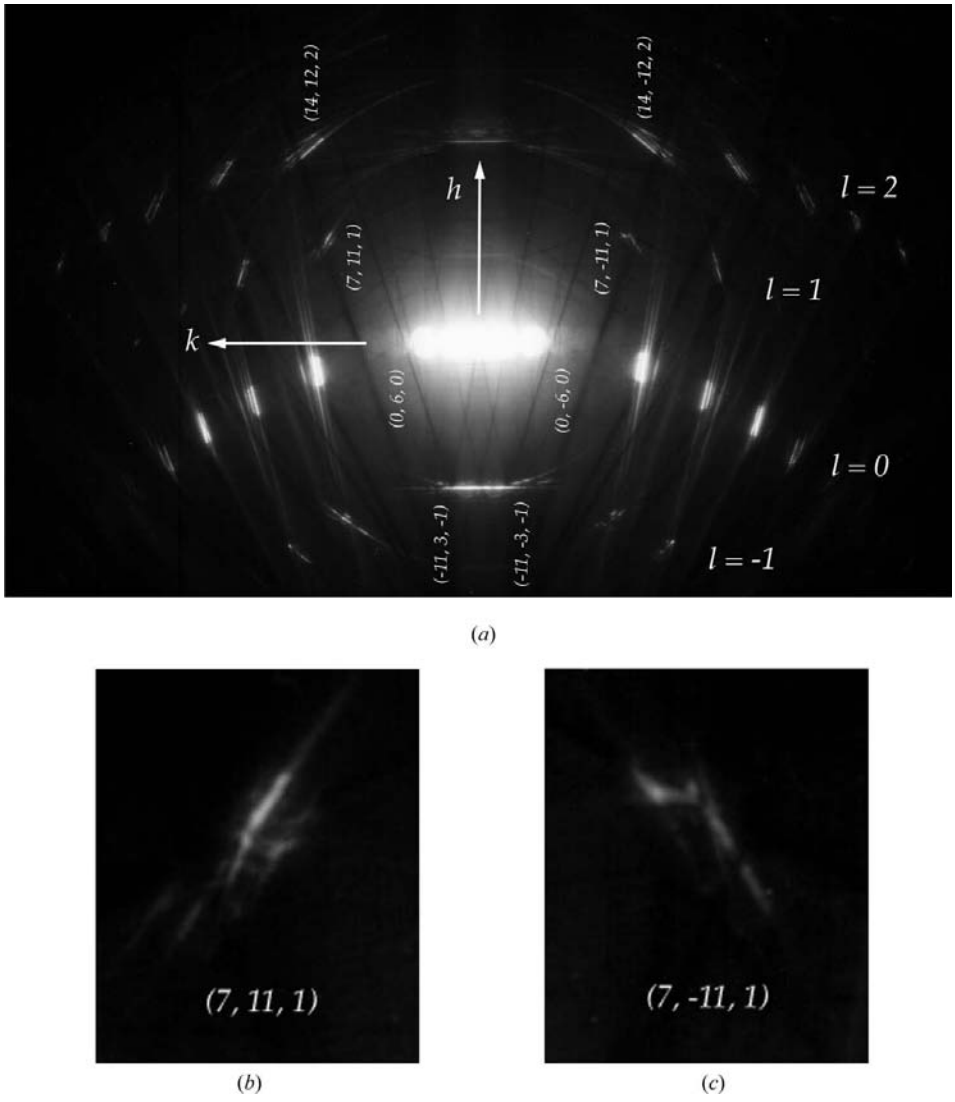

Figure 3
(*a*) CBED pattern resulting from tilting the crystal $\sim 5^\circ$ away from the [001] orientation about the $\mathbf{b}_f$ axis. (*b*) (7, 11, 1) and (*c*) (7, −11, 1) reflections from the $l = 1$ arc.

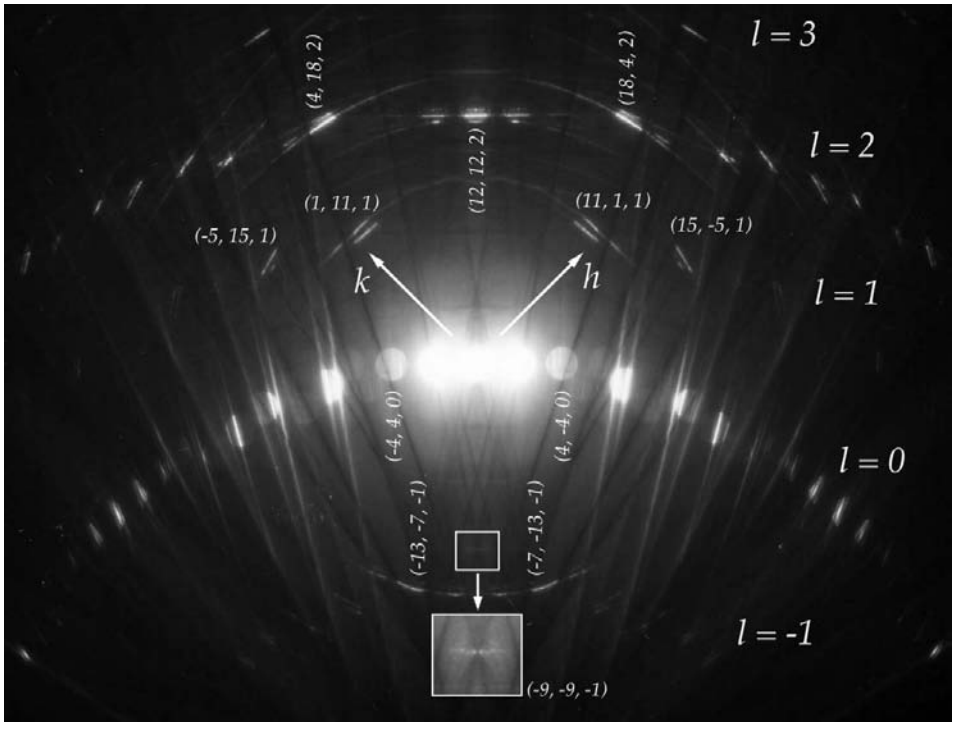

Figure 4
CBED pattern resulting from tilting the crystal $\sim 5^\circ$ away from the [001] orientation about the $\mathbf{a}_f - \mathbf{b}_f$ axis. The $(\bar{9}\bar{9}\bar{1})$ reflection from the $l = -1$ arc is enlarged and recorded at a longer exposure time to more clearly illustrate the presence of a GM band.

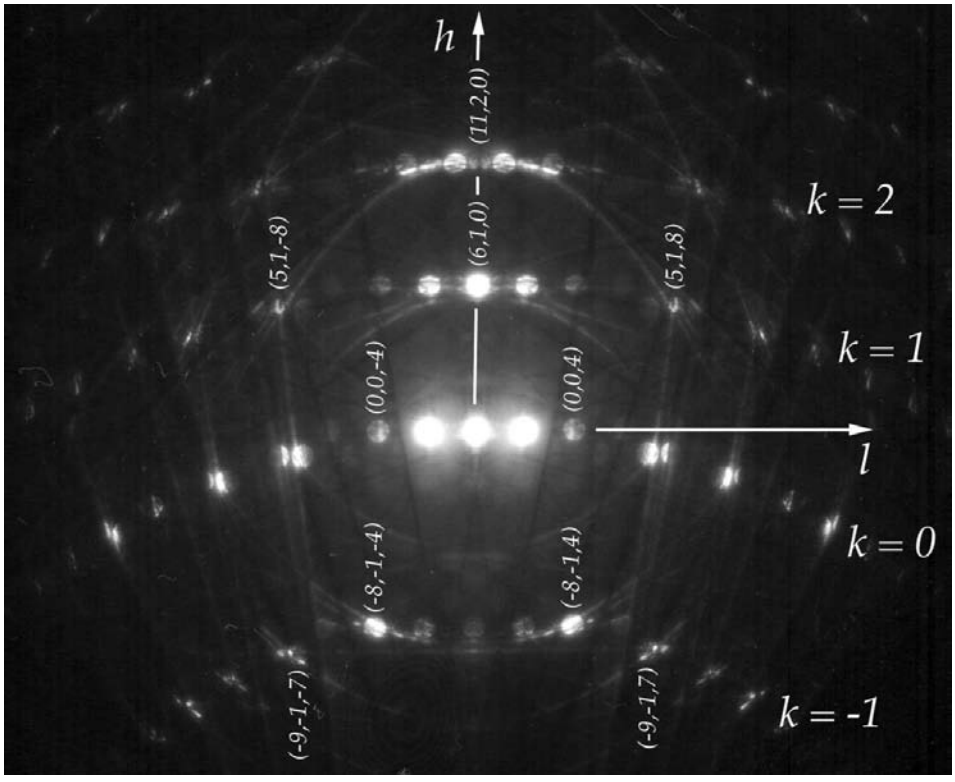

Figure 5
CBED pattern of $GdAlO_3$. The specimen has been tilted away from the [010] orientation by $\sim 6^\circ$ about the **c** axis. Indices refer to the orthorhombic *Pnma* cell (Geller & Bala, 1956).

heavy La atoms, which are essentially unmoved from their cubic sites (§2). One would therefore expect the ZOLZ to be insensitive to the small deviations from cubic symmetry that can be better observed in the odd-order HOLZ reflections. Here, the ZOLZ should not be relied upon to determine the space group. Yang *et al.* (1991) also offer a [001], bright field, large-angle CBED (LACBED) pattern which they claim shows convincing 4*mm* symmetry. This is also insensitive to small deviations from cubic symmetry as most of the intensity in their bright-field LACBED disc arises from ZOLZ scattering processes. In fact, the lower spatial resolution of LACBED compared with CBED makes thickness variation or strains across the probed region the more likely source of any symmetry breaking. A more sensitive method to observe the deviation from cubic symmetry in $LaAlO_3$ is to use the tilted HOLZ patterns described in the present work.

The pseudo-cubic angle of $LaAlO_3$ measured by XRD is 90.1° (Lehnert *et al.*, 2000), which represents a geometric distortion of $\sim 0.1\%$ in the shape of the ideal cubic unit cell. It may be possible to observe this distortion by examining clusters of HOLZ deficiency lines in the bright field disc, independent of scattering from the O atoms. This approach requires the accelerating voltage to be lowered (~ 100 kV) and/or reducing the specimen temperature to increase the visibility of the HOLZ deficiency lines. Similar work has been pursued by Midgley (1991). The author is indebted to one of the referees for suggesting the above technique.

In the case of $GdAlO_3$, there is no dispute concerning the orthorhombic *Pnma* structure. Small tilt patterns, such as those shown in Fig. 5, confirm that the mirror/glide mirror planes in this structure exist to a high level of accuracy. Such results, in the case of well char-

acterized mirror symmetries, serve to demonstrate the accuracy of the method.

Other aspects of the small tilt method are worthy of comment. Firstly, it is, potentially, very sensitive for distinguishing glide planes from screw axes. This sensitivity may be required, for example, in a structure where the majority of the atoms are glide-related but with two weakly scattering atoms in a twofold screw relation. Figs. 4 and 5 show cases where large amounts of HOLZ intensity enable mirror symmetry to be confirmed in considerable detail. Here glide mirror symmetry can be rigorously assigned. In comparison, the refined technique of Tanaka *et al.* (1983), which relies on fine HOLZ deficit lines in ZOLZ reflections to distinguish glides from screws, is less sensitive. This is apparent in Fig. 4(*c*) of their paper, where the HOLZ deficiency lines are masked by strong ZOLZ scattering. Eades (1988) has also published work on the differentiation of glides and screws using the internal disc symmetries in dark field patterns.

Secondly, the small-tilt method allows the presence or absence of GM bands in HOLZ reflections to be more easily observed. Provided sufficient tilt is used to bring a number of HOLZ rings into the field of view, such patterns allow the extinction condition associated with a glide operator to be determined and the glide translation (axial, diagonal *etc.*) to be assigned. These conditions are well illustrated in Fig. 5, where a GM band is observed in the (11,2,0) reflection, but not in the (6,1,0) reflection, uniquely determining an axial *a* glide. In contrast, at the [010] zone-axis orientation, only ZOLZ GM extinctions could be observed and this leaves the glide translation (axial or diagonal) ambiguous. It should be noted that the GM extinctions observed at the tilted orientation in Fig. 5 agree with the theoretical prediction given by Tanaka *et al.* (1988, p. 217).

A final point concerns the possible effect of crystal surfaces on the tilted HOLZ patterns. This issue has been discussed by Goodman (1974), who observed that highly tilted crystal surfaces can degrade CBED mirror symmetry, and by Eades *et al.* (1983) who came to a similar conclusion. In the present work no effects due to tilted surfaces could be observed. In the case of $LaAlO_3$, one crystal specimen was used to obtain tilted HOLZ patterns, such as Figs. 3 and 4, where the tilt away from the [001] axis was $\sim 5^\circ$. Using bright field thickness fringes taken at the exact [001] orientation, an *n*-beam thickness fringe calculation showed this crystal to be a wedge of $\sim 10^\circ$. Given the relative rotation of image and diffraction modes, it was clear that the mirror observed in Fig. 4 was approximately parallel to the wedge edge. A wedge, geometrically, contains no mirror parallel to its edge, so the excellent mirror symmetry observed in Fig. 4 shows that the CBED data in this case is unaffected by the crystal surface. Furthermore, the second mirror observed in this $LaAlO_3$ crystal specimen (discussed earlier) required a tilt of at least 45° from the orientation used to record Fig. 4. This confirms, within the qualitative scope of this experiment, that significantly tilted crystal surfaces do not affect the observed CBED symmetry.

The author wishes to gratefully acknowledge the assistance of Professor A. W. S. Johnson during the preparation of this manuscript. Helpful discussions with and encouragement from Dr M. Saunders and Dr P. A. Midgley are also acknowledged.

References

Berkstresser, G. W., Valentino, A. J. & Brandle, C. D. (1991). *J. Cryst. Growth*, **109**, 467–471.
Boulay, D. du, Ishizawa, N. & Maslen, E. N. (2004). *Acta Cryst.* C**60**, i120–i122.
Bueble, S., Knorr, K., Brecht, E. & Schmahl, W. W. (1998). *Surf. Sci.* **400**, 345–355.
Cho, S. Y., Kim, I. T. & Hong, K. S. (1999). *J. Mater. Res.* **14**, 114–119.
Derighetti, B., Drumheller, J. E., Laves, F., Müller, K. A. & Waldner, F. (1965). *Acta Cryst.* **18**, 557.
Dernier, P. D. & Maines, R. G. (1971). *Mater. Res. Bull.* **6**, 433–440.
Eades, J. A. (1988). *Microbeam Analysis*, edited by D. E. Newbury, pp. 75–80. San Francisco, USA: San Francisco Press.
Eades, J. A., Shannon, M. D. & Buxton, B. F. (1983). *Scanning Electr. Microsc.* **III**, pp. 1051–1060.
Geller, S. & Bala, V. B. (1956). *Acta Cryst.* **9**, 1019–1025.
Gjønnes, J. & Moodie, A. F. (1965). *Acta Cryst.* **19**, 65–67.
Glazer, A. M. (1972). *Acta Cryst.* B**28**, 3384–3392.
Goodman, P. (1974). *Nature*, **251**, 698–701.
Goodman, P. (2001). *International Tables for Crystallography*, Vol. B, pp. 285–306. Dordrecht: Kluwer Academic Publishers.
Howard, C. J., Kennedy, B. J. & Chakoumakos, B. C. (2000). *J. Phys. Condens. Matter*, **12**, 349–365.
Johnson, A. W. S. (1992). *International Tables for Crystallography*, Vol. C, pp. 462–463. Dordrecht: Kluwer Academic Publishers.
Lehnert, H., Boysen, H., Dreier, P. & Yu, Y. (2000). *Z. Kristallogr.* **215**, 145–147.
Marezio, M., Remeika, J. P. & Dernier, P. D. (1970). *Acta Cryst.* B**26**, 2008–2022.
Midgley, P. A. (1991). PhD thesis. University of Bristol.
Moreau, J. M., Michel, C., Gerson, R. & James, W. J. (1970). *Acta Cryst.* B**26**, 1425–1428.
Müller, K. A., Berlinger, W. & Waldner, F. (1968). *Phys. Rev. Lett.* **21**, 814–817.
Tanaka, M., Sekii, H. & Nagasawa, T. (1983). *Acta Cryst.* A**39**, 825–837.
Tanaka, M. & Terauchi, M. (1985). *Convergent-Beam Electron Diffraction.* Tokyo: Jeol-Maruzen.
Tanaka, M., Terauchi, M. & Kaneyama, T. (1988). *Convergent-Beam Electron Diffraction* II. Tokyo: Jeol-Maruzen.
Wanklyn, B. M. (1969). *J. Cryst. Growth*, **5**, 323–328.
Yang, C. Y., Huang, Z. R., Yang, W. H., Zhou, Y. Q. & Fung, K. K. (1991). *Acta Cryst.* A**47**, 703–706.